

UCSF

UC San Francisco Previously Published Works

Title

Emotional Resilience Predicts Preserved White Matter Microstructure Following Mild Traumatic Brain Injury.

Permalink

<https://escholarship.org/uc/item/0xz926k9>

Journal

Biological Psychiatry: Cognitive Neuroscience and Neuroimaging, 9(2)

Authors

Cai, Lanya

Brett, Benjamin

Palacios, Eva

et al.

Publication Date

2024-02-01

DOI

10.1016/j.bpsc.2022.08.015

Peer reviewed



HHS Public Access

Author manuscript

Biol Psychiatry Cogn Neurosci Neuroimaging. Author manuscript; available in PMC 2024 March 14.

Published in final edited form as:

Biol Psychiatry Cogn Neurosci Neuroimaging. 2024 February ; 9(2): 164–175. doi:10.1016/j.bpsc.2022.08.015.

Emotional Resilience Predicts Preserved White Matter Microstructure following Mild Traumatic Brain Injury

Lanya T. Cai^a, Benjamin L. Brett^b, Eva M. Palacios^a, Esther L. Yuh^a, Ioanna Bourla^a, Jamie Wren-Jarvis^a, Yang Wang^b, Christine Mac Donald^c, Ramon Diaz-Arrastia^d, Joseph T. Giacino^e, David O. Okonkwo^f, Harvey S. Levin^g, Claudia S. Robertson^g, Nancy Temkin^c, Amy J. Markowitz^a, Geoffrey T. Manley^a, Murray B. Stein^h, Michael A. McCrea^b, Ross D. Zafonte^e, Lindsay D. Nelson^{b,*}, Pratik Mukherjee^{a,*}, TRACK-TBI Investigators[†]

^aUniversity of California, San Francisco, CA

^bMedical College of Wisconsin, Milwaukee, WI

^cUniversity of Washington, Seattle, WA

^dUniversity of Pennsylvania, Philadelphia, PA

^eSpaulding Rehabilitation Hospital, Harvard Medical School, Boston, MA

^fUniversity of Pittsburgh Medical Center, Pittsburgh, PA

^gBaylor College of Medicine, Houston, TX

^hUniversity of California, San Diego, CA

Abstract

Background: Adult patients with mild traumatic brain injury (mTBI) exhibit distinct phenotypes of emotional and cognitive functioning identified by latent profile analysis of clinical neuropsychological assessments. When discerned early after injury, these latent clinical profiles have been found to improve prediction of long-term outcomes from mTBI. The present study hypothesized that white matter (WM) microstructure is better preserved in an emotionally resilient (ER) mTBI phenotype compared with a neuropsychiatrically distressed (ND) mTBI phenotype.

Methods: The present study used diffusion MRI to investigate and compare WM microstructure in major association, projection, and commissural tracts between the two phenotypes and over time. Diffusion MR images from 172 mTBI patients were analyzed to compute individual diffusion tensor imaging (DTI) maps at 2 weeks and 6 months postinjury.

*Co-correspondence: **Lindsay D. Nelson**, Neurosurgery, 8701 Watertown Plank Rd., Milwaukee, WI 53226, (414)805-3666, linelson@mcw.edu, **Pratik Mukherjee**, Radiology, 185 Berry St., San Francisco, CA 94158, (415)353-8972 ext. 23852, pratik.mukherjee@ucsf.edu.

[†]A complete list of the TRACK-TBI consortium is in the Acknowledgements.

Publisher's Disclaimer: This is a PDF file of an article that has undergone enhancements after acceptance, such as the addition of a cover page and metadata, and formatting for readability, but it is not yet the definitive version of record. This version will undergo additional copyediting, typesetting and review before it is published in its final form, but we are providing this version to give early visibility of the article. Please note that, during the production process, errors may be discovered which could affect the content, and all legal disclaimers that apply to the journal pertain.

Results: By comparing the DTI parameters between the two phenotypes at global, regional, and voxel levels, the present study showed that the ER patients have higher axial diffusivity (AD) compared to their ND counterparts early after mTBI. Longitudinal analysis revealed greater compromise of WM microstructure in ND patients, with greater decrease of global AD and more widespread decrease of regional AD during the first 6 months after injury compared to their ER counterparts.

Conclusions: These results provide neuroimaging evidence of WM microstructural differences underpinning mTBI phenotypes identified from neuropsychological assessments and show differing longitudinal trajectories of these biological effects. These findings suggest diffusion MRI can provide short- and long-term imaging biomarkers of resilience.

Keywords

traumatic brain injury; neuropsychology; neuroimaging; diffusion MRI; DTI; resilience

Introduction

Traumatic brain injury (TBI) affects tens of millions of people worldwide annually, the vast majority classified as mild TBI (mTBI). Postinjury neuropsychiatric conditions include posttraumatic stress disorder (PTSD), anxiety disorders, and major depressive disorder (MDD) (1, 2). These can compromise quality of life, including decreased functional capacity, such as the ability to return to work (3), and drastically impact the life of caregivers and surrounding community (4–7).

Although classification systems for TBI severity exist based on Glasgow Coma Scale (GCS) and head computed tomography (CT) (8–11), patients exhibit wide variation in postinjury recovery unexplained by TBI severity. For example, two patients who sustain an injury of comparable severity, for example, mTBI defined as GCS score 13–15, may or may not manifest neuropsychiatric difficulties postinjury. They may experience different clinical symptom presentations, e.g., PTSD versus MDD (12–14). It is therefore critical to better understand neuropsychiatric symptoms following mTBI by investigating changes that underlie risk for these postinjury disabilities.

Using latent profile analysis, Brett et al. (2021) recently showed that 1,757 TBI participants (mild to severe) can be classified into clinically distinct phenotypes based on emotional and cognitive functioning at two-weeks postinjury assessed using twelve different tests included in the NIH Common Data Elements (15). Latent profile analysis is a mixture modeling method that assumes the presence of underlying, unmeasured phenotypes (subgroups of participants) that can be identified from distinct patterns of observed variables (here, symptom and cognitive performance measures). These acute TBI phenotypes strongly predicted 6-month postinjury outcomes across functional, clinical, and quality of life (QoL) domains using standard tests different than those used to define the phenotypes. A four-group solution included two distinct profiles that differentiated those experiencing postinjury neuropsychiatric distress (ND; n=350 patients) from those exhibiting emotional resilience (ER; n=419 patients). Another two profiles were characterized by cognitive difficulties (n=368 patients) versus cognitively resilient (n=620 patients). The ER group stood out as

having the best prognosis for functional, clinical, and QoL outcomes at 6-months postinjury, while the ND group had the worst prognosis.

Resilience is a salient area of interest in neuroscience, psychology, and sociology, encompassing the capacity to respond to adverse life and health experiences with adaptation, flexibility, and persistence (16, 17). Given the influence of emotional resilience on 6-month outcomes post-TBI, it is critical to understand its biological mechanisms (15). This represents the emerging viewpoint that devising better TBI rehabilitation requires understanding not just “what the injury brings to the brain” but also “what the brain brings to the injury”.

Diffusion tensor imaging (DTI) has been widely applied to characterize white matter (WM) pathology in mTBI because of its sensitivity to diffuse axonal injury (DAI) (18–22). Schmidt et al. (2021) recently found using DTI that resilience-promoting factors (e.g., community support, close interpersonal relationships) were associated with intact WM microstructural integrity in a small adolescent sample of all-severity TBI (23). Other studies indicate that WM microstructure correlates with resilience in adolescents (24, 25). WM structural network efficiency derived from diffusion MRI (dMRI) predicts resilience to cognitive decline in adults at risk for Alzheimer’s disease (26). Conversely, reduced integrity of WM tracts has been observed in those with psychiatric diagnoses or higher levels of psychiatric symptomatology (27). Taken together, WM microstructure represents a promising biological marker to elucidate emotional resilience versus neuropsychiatric distress following mTBI.

Our objectives were to investigate: 1) WM differences in ER versus ND phenotypes in acute mTBI, and 2) longitudinal WM changes across the two phenotypes up to 6 months postinjury. We studied a subset of the TRACK-TBI participants examined by Brett et al. (2021) ages 17–60 years that met criteria for mTBI and underwent DTI at both two weeks and 6 months postinjury. We focused on the ER and ND groups because they had the greatest divergence in recovery after mTBI (15) and because emotional resilience has significance in many other neuropsychiatric disorders. Figure 1 shows a schematic of hypothesized roles of resilience and DAI and expected observations.

We hypothesized that the ER group would exhibit greater WM integrity acutely (2 weeks) post-TBI and exhibit less decrease at 6 months postinjury. Axial diffusivity (AD) was selected as the primary DTI metric since it represents the component of WM microstructural integrity along the principal axonal fiber orientation. A higher AD is often linked with greater WM microstructural integrity and decrease of AD over time is often linked with WM deterioration. Its response to TBI is more monophasic from the acute to chronic phase of injury than other commonly used DTI metrics such as fractional anisotropy (FA) and mean diffusivity (MD) in both animal experimental models (28) and human studies (29).

Methods and Materials

Participants

The present study included mTBI participants from the Transforming Research and Clinical Knowledge in TBI (TRACK-TBI) study (30). The participants were enrolled between 2014

and 2018 at 11 academic Level 1 trauma centers across the United States within 24 hours of injury and were evaluated in the Emergency Department or hospital inpatient unit. All participants offered written consent to the study protocol approved by the Institutional Review Board (IRB) at University of California, San Francisco and the IRBs at other participating sites. Additional enrollment and inclusion criteria are reported in the supplements. Of the 1,132 mTBI patients in the cohort, 391 from 17–60 years of age underwent MRI at both 2-week and 6-month time points. Of these 391 patients, 94 were classified as ER and 78 were classified as ND based on the latent profile analysis of their responses to a comprehensive battery of neuropsychological assessments/inventories at two-weeks postinjury (15). The ER and ND phenotypes were not equivalent to any diagnosis from traditional approaches, e.g., Diagnostic and Statistical Manual (DSM) and International Classification of Diseases (ICD). In addition, a demographically matched control group of 148 uninjured volunteers was enrolled using the same inclusion and exclusion criteria except for those related to head injury.

Clinical Outcomes at 6 months

Patients were assessed at 6 months postinjury. The Glasgow Outcome Scale-Extended (GOSE) score measures diverse changes in daily functioning after traumatic injuries; a score <8 indicates incomplete recovery (9, 30–33). TBI-related symptoms were assessed using the Rivermead Post Concussion Symptoms Questionnaire (RPQ, ranges from 0–64), with higher scores indicating more severe injury-related symptoms (34).

MRI Acquisition

Whole-brain MRI with diffusion sequences were conducted using 3T MR scanners with phased-array head radiofrequency coils. Measures were standardized across sites by using a consistent acquisition protocol and a calibration process with a traveling diffusion phantom and human volunteers (35). For each patient at each time point, multi-slice single-shot spin-echo echo-planar pulse sequences were acquired at $b=1300 \text{ s}\cdot\text{mm}^{-2}$ for 64 diffusion-encoding directions and at $b=0 \text{ s}\cdot\text{mm}^{-2}$ for 8 acquisitions, with slices 2.7-mm thick and no gaps, a matrix of 128×128 , and an FOV of 350 mm. The resulting voxel size is 2.7-mm in all three dimensions.

DTI Processing and Analysis

DTI preprocessing and Tract-Based Spatial Statistics (TBSS) were performed using the Functional MRI of the Brain Software Library (FSL) (36). DTI parameters (FA, MD, AD, and RD) were calculated after correction of susceptibility and eddy current induced distortions by registering each volume to the b_0 volume, without using reverse phase-encoding acquisitions. Individual FA maps were skeletonized and registered to the FMRIB58 FA template in MNI152 standard space. Global mean DTI parameters were computed over the entire brain WM skeleton. Region-of-interest (ROI) values of WM tracts were obtained by masking the individual WM skeletons with JHU ICBM-DTI-81 WM Labeled Atlas (37) regions in MNI152 space and averaging across voxels in each region. Whole-brain voxelwise group comparison was implemented with permutation testing and corrected for multiple voxelwise comparisons using threshold-free cluster enhancement at p 0.05 (38).

Statistical analyses

For comparing global AD between ER and ND patients: (1) an unpaired t-test was performed to evaluate the significance of differences between groups at each time point; (2) a paired t-test was performed to evaluate the significance of within-group longitudinal differences; (3) an unpaired t-test was performed to evaluate the phenotype differences of longitudinal changes. For the phenotype comparison of regional DTI parameters at each time point, bilaterally measured regions were averaged, then an unpaired heteroscedastic t-test was used for statistical inference, and Cohen's d was computed to evaluate the effect size. The Benjamini-Hochberg FDR adjusted p -value was computed to correct for multiple comparisons (39). To explore the longitudinal changes in regional AD, a paired t-test was performed to evaluate the significance of within-group longitudinal change, and a repeated-measures ANOVA was performed with *Time* set as the within-subject factor, *Phenotype* set as the between-subject factor (excluding control group for lacking phenotype assignments), and an interactive term of *Phenotype: Time*. For the comparison of 6-month clinical outcomes, an unpaired heteroscedastic t-test was performed.

Results

The demographic, clinical, and CT results of the ER and ND patients are provided in Supplementary Table S1. There was no age difference between ER (36.1 ± 13.4 years) and ND (35.1 ± 11.7 years). ND had twice as many women (43.6%) as ER (21.3%). ER had more years of education (14.9 ± 2.8) than ND (12.9 ± 2.1). There were trends towards higher rates of loss of consciousness (LOC), posttraumatic amnesia (PTA), and acute TBI findings on CT in ER than ND. There was also a trend towards a higher rate of prior neuropsychiatric diagnosis in ND.

Results comparing WM microstructure between ER and ND are presented in ascending order of spatial resolution, from global WM (Figure 2) to regional WM tracts (Figure 3, Tables 1–3) to voxelwise WM (Figure 4).

Global axial diffusivity

For both timepoints, ND had lower global AD than ER ($p=0.045$ at 2 weeks, $p=0.005$ at 6 months). ER showed no significant longitudinal change ($p=0.45$, Cohen's $d=0.08$) whereas ND exhibited a significant longitudinal decrease in global AD ($p=0.003$, Cohen's $d=0.35$). The longitudinal global AD change in ND participants was greater than their ER counterparts ($p=0.043$, Cohen's $d=0.31$).

Phenotype difference of regional DTI

To identify which WM tracts contributed most to this global AD difference between ER and ND groups, *post hoc* region of interest (ROI) analysis was performed at two weeks and six months, correcting for multiple comparisons (Tables 1–2; see captions for tract abbreviations). At two weeks, ND had significantly lower AD than ER in FX and SCP. The AD group differences increased from 2 regions at two weeks to 13 regions at six months. The ND group showed significantly lower AD in association tracts (EC, FXST, SFO, SS, and UNC) and projection tracts of the internal capsule (ALIC/PLIC/RLIC), as well

as brainstem (CP and ML). Regions with lower AD in the ND group at two weeks postinjury showed increased effect size by six months (FX and SCP).

Longitudinal change of regional axial diffusivity

Table 3 reports longitudinal change of regional AD using repeated-measures ANOVA. Figure 3 reveals that ND had significant longitudinal reductions of AD in 7 regions, while ER only had them in PLIC and GCC. The ER group also trended towards increased AD in SS, PCR, and PTR. No significant change was found in uninjured controls for any of the tracts.

ND patients showed deterioration of WM microstructure as progressively reduced AD in more WM regions (Table S2) than ER patients, in whom significant interval AD decreases were limited to the internal capsule and GCC (Table S3).

Voxelwise analysis of axial diffusivity

Significant voxelwise AD differences between ER and ND at two-weeks postinjury were mostly in central regions, which extended to more peripheral and posterior regions over the following six months (Figure 4), such as PCR and PTR where longitudinal ROI analysis showed that AD was trending upwards in ER but was significantly decreasing in ND (Fig. 3). We also performed the longitudinal voxelwise *t*-statistics within each group but did not find any significant changes after multiple voxelwise comparison correction.

Clinical outcomes at 6 months

ER patients predominantly demonstrated full functional recovery (GOSE=8), whereas ND patients had significantly lower GOSE scores ($p<0.001$) representing incomplete recovery, with a shallow distribution over the range of 4 – 8 (Figure 5A). Most ER patients had zero RPQ (Figure 5B), implying no remaining TBI symptoms (34), whereas ND patients had significantly higher RPQ over a wide distribution ($p<0.001$).

Discussion

This prospective, natural history study of mTBI patients is the first, to our knowledge, to interrogate neural pathways of resilience associated with distinct neuropsychiatric phenotypes postinjury. WM microstructural differences between ER and ND phenotypes of mTBI were clearly identified at two-weeks postinjury, and became larger and more widespread at six months. DTI revealed lower WM AD and therefore possibly reduced microstructural integrity in ND patients compared with their ER counterparts. This difference increased from two to 13 major WM tracts during the first six months postinjury, indicating that greater neuropsychiatric distress interacts with injury-related processes to confer worse biological responses to mTBI, whereas greater emotional resilience may serve as a protective factor, both early and especially later during mTBI recovery. These findings support the novel phenotypic classification of Brett et al. (2021), with a striking group difference in six-month outcomes. Whereas the majority of the ER group identified early after injury had little or no long-term disability or symptoms, the majority of the ND group had poor long-term outcomes. This cannot be explained by differences in standard

clinical and CT measures of injury severity, all of which indicated more severe TBI in the ER group rather than the ND group (Table S1). This implies that emotional resilience is a major determinant of recovery after mTBI, or that yet-to-be-determined (likely non-injury) factors drive long-term emotional and neurobiological outcomes. Given the high prevalence of mTBI worldwide, elucidating the neuroscientific underpinnings of resilience and leveraging this knowledge to improve diagnosis and treatment of mTBI patients should be a major focus of research, especially if these neural mechanisms are also shared with other neurological and psychiatric disorders.

The evident association between mTBI phenotypes and WM integrity implicates particular neurobiological mechanisms and may prove useful as diagnostic, prognostic and/or predictive biomarkers for clinical trials and patient management. The ER and ND phenotypes contrast along multiple psychiatric symptom dimensions post-TBI, including internalizing factors (depression, anxiety, fear) and somatic factors (sleep problems, physical difficulty, and pain) (40). Distinct patterns of WM changes associated with these symptoms may contribute to the feature segregation between phenotypes. Axonal damage of tracts related to emotional functions may predict neuropsychiatric manifestations after TBI. Aldossary et al. (2019) showed that severe TBI patients with DAI were more likely to exhibit personality changes, aggression, and MDD, implicating emotional regulation neurotransmitter circuits of the frontal and anterior temporal lobes (41). We found greater reduction of diffusivity in SFO, SLF, UNC, and FX, corroborating the hypothesized disrupted neurotransmitter circuits.

In the broader neurosciences, studies have linked limbic and neocortical association tracts with internalizing mental illness. The FX and cingulum are associated with emotional dysfunction in bipolar disorder (42). Decreased UNC integrity was found in MDD (43). Jenkins et al. (2016) studied shared WM microstructural abnormalities of patients across various emotion disorders using DTI and found reduced FA in UNC and SLF (44). This is germane to the current study, as the classification of ER and ND was based on a transdiagnostic approach comprising various dimensions of internalizing and somatic psychiatric symptoms. We observed significantly lower AD in FX, UNC, and SLF in ND patients versus ER patients, concordant with previous findings, and lower AD of the ND group in other neocortical association tracts, including EC, SFO, and SS, by 6 months postinjury.

Compromised WM microstructure of commissural and projection tracts might also correlate with emotional deficits. Jenkins et al. (2016) reported reduced FA in the GCC, ATR and SCR (44). Corpus callosum and ALIC has lower FA in MDD patients relative to controls (45). We observed cross-sectional and/or longitudinal differences of AD in ND versus ER in the ALIC, but also in many more tracts at six months postinjury. Interestingly, posterior fibers of the PCR, PTR and SS in ER patients trended towards an increased AD over time, suggesting possible recovery of axonal integrity.

Damage to the cerebellum might be important for the deleterious effects of mTBI since it is sensitive to timing and has been postulated as the hub within the network for attentional prediction (46,47). AD of the cerebellar peduncles is reduced in both collegiate athletes

and Emergency Department patients with mTBI compared with controls (48). In the current study, AD of the SCP was reduced in ND versus ER at both time points. Both cerebral and cerebellar peduncles (CP, ICP) showed reduction of AD over time in ND but not ER patients. Therefore, microstructural plasticity of cerebellar input/output WM pathways via its peduncles, which is vital for maintaining precise spike timing (49–51), may be an important mechanism of mTBI resilience in addition to causing post-concussive symptoms when damaged. Hence, those with greater preinjury microstructural integrity of the cerebellar peduncles might tolerate the same severity of injury with fewer symptoms and less disability than those without this advantage.

These neurobiological correlates of ER versus ND are dynamic over time, leading to different potential interpretations at two weeks versus six months postinjury. Higher AD at two weeks postinjury may indicate that ER patients had less severe injury to axonal density and less disruption of axonal orientation coherence relative to ND patients. Higher AD six months later may indicate that the ER patients had recovered better and/or that the ND patients had more WM degeneration. However, a high AD does not necessarily mean better WM microstructural integrity in the ER patients at two weeks. Acute neural deformation edema can also have a transient effect on local AD, which may explain the finding by Brett et al. (2021) that the latent profiles did not intuitively cohere with TBI severity scores (15). They found that lower admission GCS (<13) were observed more commonly in ER (7.9%) than ND (5.5%), indicating that ER patients tended to have greater injury severity. ND had a higher percentage of women than ER; however, sex differences cannot explain the different WM AD changes between ER and ND across the two timepoints. Interestingly, differences of longitudinal AD changes between ER and ND were evident in the ROI analysis but not in the voxelwise analysis, likely because voxelwise analysis has more stringent multiple comparison corrections and thus lower statistical power.

Resilience can exist prior to TBI as a premorbid host factor. A minority of ER and ND patients reported preinjury psychiatric problems which were only slightly more common in the ND group. McCauley et al. (2013) evaluated preinjury clinical/functional resilience in mTBI patients *post hoc* by using the Connor-Davidson Resilience Scale (CDRS) based on the patients' memory of their functioning a month before the injury (52). They observed that preinjury resilience and preinjury depressed mood predicted postinjury outcomes. Another study of post-TBI resilience using the CDRS found that premorbid host factors (e.g., minority group membership, preinjury substance abuse, and higher levels of anxiety and disability) were related to reduced resilience during the first year postinjury (53). TBI patients with MDD are more likely to have a history of mood and anxiety disorders than TBI patients without depression, linking lower resilience to emotional deficits after TBI (54). Premorbid somatization symptoms influence clinical recovery after sport related concussion (55). Manic symptoms post-TBI were more frequent in patients with a positive family history of bipolar disorder, suggesting that neuropsychiatric risk factors existed preinjury (56). An earlier study also showed a strong relationship between severe mental illness post-TBI and family histories of schizophrenia or bipolar disorder (57).

Alternatively, post-TBI resilience may develop in response to injury. Schmidt et al. (2021) suggested that the protective effects of resilience in adolescent TBI patients may be a

result of less disrupted WM tracts combined with quality of support from family and caregivers (23). Accordingly, resilience may be responsive and not just innate, although a positive correlation may exist between preinjury resilience and superior family/caregiver environments that can further enhance resilience postinjury. Task-oriented coping and perceived social support, but not premorbid intelligence, predicted high resilience on the CDRS post-TBI (58).

Since premorbid resilience cannot be ascertained in most TBI study designs, our study is unable to distinguish between altered microstructural WM integrity due to DAI and that due to resilience. The conventional explanation for the group differences (Figure 1A) is that more severe DAI accounts for the lower WM integrity at two weeks in the ND group and that continued Wallerian axonal degeneration produces the widening gap between ND and ER at six months. However, there is no clinical evidence for greater DAI in the ND group, rather, the ER group trended toward higher proportions of LOC, PTA, and acute intracranial injury on CT scanning, which are all factors associated with greater injury severity. The alternate explanation (Figure 1B) is that differences in preinjury resilience accounts for the differences in DTI metrics at two weeks and that persistent adaptive behaviors among the ER group, versus maladaptive behaviors among the ND group, explain the relatively preserved WM microstructure of ER patients by 6 months postinjury, similar to that of the uninjured controls, versus the deteriorating WM integrity of the ND patients. This view is consistent with the finding of higher educational levels in the ER group. Rates of premorbid psychopathology did not differ between ER and ND, indicating that this construct is not simply due to pre-existing neuropsychiatric history. Furthermore, the greatest variation in WM microstructure between the two groups were in tracts implicated in resilience and neuropsychiatric function, as opposed to the more uniform and diffuse group differences that would be postulated by the DAI hypothesis. However, there are likely interactions between DAI and preinjury resilience during the recovery from mTBI, since DAI can affect WM tracts required for clinical/functional resilience and, in turn, resilience can promote adaptive responses to injury that might potentially prevent further WM degeneration induced by DAI. This latter interaction is supported by the one-year follow-up DTI data from a recent pilot study of resilience-promoting factors in adolescents with complicated mild, moderate, and severe TBI (23).

Given the enlarging differences in WM microstructure between ER and ND over time, improving post-TBI intervention is urgent, demanding clear identification of modifiable factors. Emergency Department mTBI patients frequently receive limited education and follow-up care (59). Variation in TBI clinical care practices conceivably contributes to resilient versus adverse clinical and neurobiological outcomes. Advancing mTBI biological and phenotypic classification is critical to better precision medicine treatment approaches, since more precisely and accurately characterizing population heterogeneity will help ensure interventions are tailored to the unique needs and preferences of individual patients (30, 60, 61). Incorporating neuroscience-informed resilience theory and positive psychology into TBI rehabilitation promises to improve long-term life quality (62–65). Patients' perception of the injury might lead to differentiated neuropsychiatric outcomes (3). Postinjury social and environmental challenges also have psychological impacts. For example, a patient and family may be unable to work to their full capacity postinjury, which consequently stretches

their financial resources (66). Professional guidance should be integrated into rehabilitation to support coping with all these stressors (67).

Limitations and Future Directions

To control for all potential confounding factors (genetics, sex, education, lifestyles, socioeconomic) would have required a larger sample size. More studies would help to determine the effect of these different demographic characteristics. DTI data from two timepoints were inadequate to quantify the effect of acute edema on AD. Future studies incorporating earlier imaging time points as well as more advanced diffusion models (e.g., NODDI) would help elucidate these acute effects of TBI.

TBSS has limited anatomical specificity, due to its reliance on FA and neglecting orientation information in the diffusion tensor (68). Also, the impact of heterogeneity in image acquisition on the results (e.g., due to scanner types) might have been reduced by advanced harmonization methods.

Regarding interpretation of the results, the reported effect sizes are not large enough to predict the outcomes of individual patients. Also, the present analyses cannot determine if particular neuropsychiatric factors (e.g., sleep, depression, anxiety, fear, sleep problems, physical difficulty, pain) were predominantly associated with AD to inform treatment recommendations. These limitations should inspire future hypothesis-driven investigations with more advanced diffusion MRI acquisition and analysis methodology.

Supplementary Material

Refer to Web version on PubMed Central for supplementary material.

Acknowledgements

This paper is in memory of our co-author Dr. Harvey S. Levin who was a pioneer in the application of neuroimaging and neuropsychology to the study of mTBI, including the role of resilience in mTBI patient outcomes. Regarding ICJME authorship criteria, we note that, due to his illness, Dr. Levin was not able to approve the final submitted version of this manuscript.

The TRACK-TBI study is sponsored by the U.S. National Institutes of Health, National Institute of Neurologic Disorders and Stroke (Grant U01 NS086090), US Department of Defense (W81XWH-14-2-0176); Abbott Laboratories, One Mind. Abbott Laboratories is supported by the US Army Medical Research and Development Command, 810 Schreider St. Fort Detrick, MD 21702, Contract W81XWH-17-C-0079. Dr. Nelson's effort was supported by NINDS grant # R01 NS110856. Dr. Brett's effort was supported by NIA grant # K23 AG073528-01.

A complete list of the TRACK-TBI consortium is provided here:

University of California, San Francisco: Adam R Ferguson, Geoffrey T Manley, Amy J Markowitz, Pratik Mukherjee, Sabrina R Taylor, John K Yue, Esther L Yuh

Barrow Neurological Institute: Ruchira Jha

Baylor College of Medicine: Shankar Gopinath, Claudia S Robertson

Harvard University / Spaulding Rehabilitation Center: Joseph T Giacino

Medical College of Wisconsin: Michael McCrea, Lindsay D Nelson

Hospital of the University of Pennsylvania: Ramon Diaz-Arrastia

University of California, San Diego: Sonia Jain, Murray B Stein

University of Cincinnati | UC Gardner Neuroscience Institute: Laura B Ngwenya

University of Maryland Medical Center: Neeraj Badjatia, Rao Gullapalli

University of Michigan: Frederick K Korley

University of Pittsburgh Medical Center | Brain Trauma Research Center: David O Okonkwo, Ava M Puccio

University of Texas at Austin: David Schnyer

UT Southwestern Medical Center: Christopher Madden

University of Utah: Ramesh Grandhi

University of Washington: C Dirk Keene, Christine L Mac Donald, Nancy R Temkin

Virginia Commonwealth University Medical Center: Randall Merchant

Disclosures

Dr. Yuh had a patent for USPTO No. 62/269,778 pending. Dr. Manley received grants from the NINDS during the conduct of the study; research funding from the US Department of Energy, grants from the DoD, research funding from Abbott Laboratories, grants from the National Football League Scientific Advisory Board, and research funding from One Mind outside the submitted work; in addition, Dr. Manley had a patent for Interpretation and Quantification of Emergency Features on Head Computed Tomography issued. He served for 2 seasons as an unaffiliated neurologic consultant for home games of the Oakland Raiders; he was compensated \$1500 per game for 6 games during the 2017 season but received no compensation for this work during the 2018 season. Dr. Stein received personal fees from Aptinyx, Bionomics, Janssen, and Neurocrine; as well as personal fees and stock options from Oxeia Biopharmaceuticals outside the submitted work. Dr. Diaz-Arrastia received personal fees and research funding from Neural Analytics Inc and travel reimbursement from Brain Box Solutions Inc outside the submitted work. Dr. Goldman received personal fees from Amgen, Avanir Pharmaceuticals, Acadia Pharmaceuticals, Aspen Health Strategy Group, and Celgene outside the submitted work. Dr. Kreitzer received personal fees from Portola outside the submitted work. Dr. Mukherjee received grants from GE Healthcare and nonfinancial Head Health Initiative outside the submitted work; in addition, Dr. Mukherjee had a patent for USPTO No. 62/269,778 pending. Dr. Rosand received personal fees from Boehringer Ingelheim and New Beta Innovations outside the submitted work. Dr. Zafonte received royalties from Oakstone for an educational CD (Physical Medicine and Rehabilitation: a Comprehensive Review) and Demos publishing for serving as coeditor of Brain Injury Medicine. Dr. Zafonte serves or served on the scientific advisory boards of Myomo, Oxeia Biopharma, Biodirection, and Elminda. He also evaluates patients in the MGH Brain and Body-TRUST Program, which is funded by the National Football League Players Association. Dr. Zafonte served on the Mackey White Committee. The other authors report no biomedical financial interests or potential conflicts of interest.

None of these funding organizations influenced the scientific content of this paper.

References

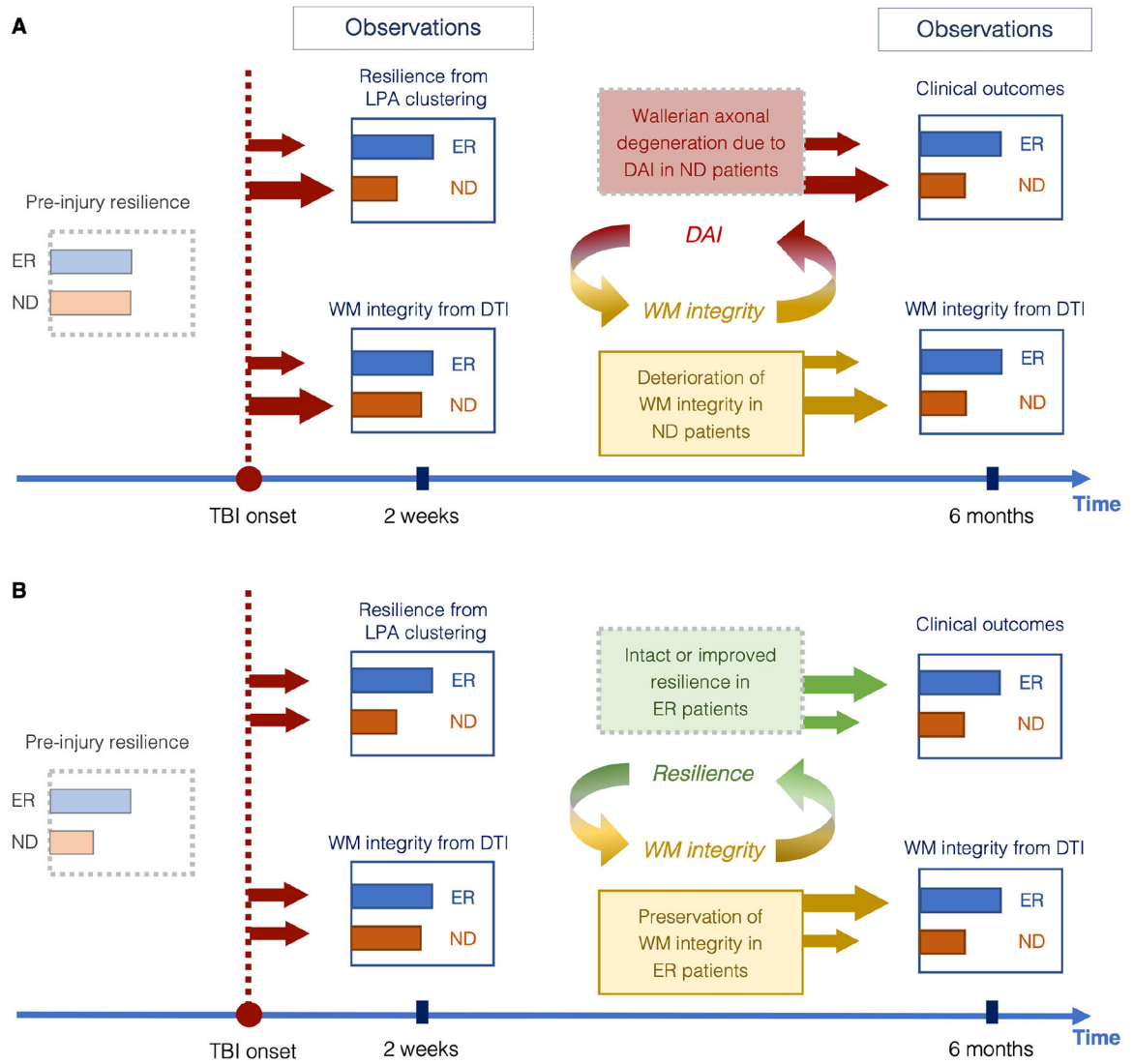
1. Bryant RA, O'Donnell ML, Creamer M, McFarlane AC, Clark CR, Silove D, 2010. The psychiatric sequelae of traumatic injury. *American Journal of Psychiatry* 167, 312–320. [PubMed: 20048022]
2. Riggio S, 2011. Traumatic brain injury and its neurobehavioral sequelae. *Neurologic Clinics* 29, 35–47. [PubMed: 21172569]
3. Dilley M, Avent C, 2011. Long-term neuropsychiatric disorders after traumatic brain injury. *Psychiatric Disorders—Worldwide Advance*. Uehara T (ed). InTech Publishing: London, 301–328.
4. Gould KR, Ponsford JL, Johnston L, Schönberger M, 2011. Predictive and associated factors of psychiatric disorders after traumatic brain injury: a prospective study. *Journal of neurotrauma* 28, 1155–1163. [PubMed: 21476784]
5. Diaz AP, Schwarzbald ML, Thais ME, Hohl A, Bertotti MM, Schmoeller R, Nunes JC, Prediger R, Linhares MN, Guarnieri R, et al. , 2012. Psychiatric disorders and health-related quality of life after severe traumatic brain injury: a prospective study. *Journal of Neurotrauma* 29, 1029–1037. [PubMed: 22111890]

6. Haagsma JA, Scholten AC, Andriessen TM, Vos PE, Van Beeck EF, Polinder S, 2015. Impact of depression and post-traumatic stress disorder on functional outcome and health-related quality of life of patients with mild traumatic brain injury. *Journal of neurotrauma* 32, 853–862. [PubMed: 25320845]
7. Scholten AC, Haagsma JA, Cnossen MC, Olf M, Van Beeck EF, Polinder S, 2016. Prevalence of and risk factors for anxiety and depressive disorders after traumatic brain injury: a systematic review. *Journal of neurotrauma* 33, 1969–1994. [PubMed: 26729611]
8. Teasdale G, Jennett B, 1974. Assessment of coma and impaired consciousness: a practical scale. *The Lancet* 304, 81–84.
9. Jennett B, Snoek J, Bond M, Brooks N, 1981. Disability after severe head injury: observations on the use of the glasgow outcome scale. *Journal of Neurology, Neurosurgery & Psychiatry* 44, 285–293. [PubMed: 6453957]
10. Murray GD, Butcher I, McHugh GS, Lu J, Mushkudiani NA, Maas AI, Marmarou A, Steyerberg EW, 2007. Multivariable prognostic analysis in traumatic brain injury: results from the impact study. *Journal of neurotrauma* 24, 329–337. [PubMed: 17375997]
11. Menon DK, Schwab K, Wright DW, Maas AI, et al. , 2010. Position statement: definition of traumatic brain injury. *Archives of physical medicine and rehabilitation* 91, 1637–1640. [PubMed: 21044706]
12. Stein MB, McAllister TW, 2009. Exploring the convergence of posttraumatic stress disorder and mild traumatic brain injury. *American Journal of Psychiatry* 166, 768–776. [PubMed: 19448186]
13. Nelson LD, Kramer MD, Patrick CJ, McCrea MA, 2018. Modeling the structure of acute sport-related concussion symptoms: a bifactor approach. *Journal of the International Neuropsychological Society* 24, 793–804. [PubMed: 30079858]
14. Agtarap S, Campbell-Sills L, Thomas ML, Kessler RC, Ursano RJ, Stein MB, 2019. Postconcussive, posttraumatic stress and depressive symptoms in recently deployed us army soldiers with traumatic brain injury. *Psychological assessment* 31, 1340. [PubMed: 31380697]
15. Brett BL, Kramer MD, Whyte J, McCrea MA, Stein MB, Giacino JT, Sherer M, Markowitz AJ, Manley GT, Nelson LD, et al. , 2021. Latent profile analysis of neuropsychiatric symptoms and cognitive function of adults 2 weeks after traumatic brain injury: findings from the track-tbi study. *JAMA network open* 4, e213467–e213467. [PubMed: 33783518]
16. Southwick SM, Bonanno GA, Masten AS, Panter-Brick C, Yehuda R, 2014. Resilience definitions, theory, and challenges: interdisciplinary perspectives. *European journal of psychotraumatology* 5, 25338.
17. Silverman AM, Verrall AM, Alschuler KN, Smith AE, Ehde DM, 2017. Bouncing back again, and again: a qualitative study of resilience in people with multiple sclerosis. *Disability and Rehabilitation* 39, 14–22. [PubMed: 26878245]
18. Bazarian JJ, Zhong J, Blyth B, Zhu T, Kavcic V, Peterson D, 2007. Diffusion tensor imaging detects clinically important axonal damage after mild traumatic brain injury: a pilot study. *Journal of neurotrauma* 24, 1447–1459. [PubMed: 17892407]
19. Lipton ML, Gulko E, Zimmerman ME, Friedman BW, Kim M, Gellella E, Gold T, Shifteh K, Ardekani BA, Branch CA, 2009. Diffusion-tensor imaging implicates prefrontal axonal injury in executive function impairment following very mild traumatic brain injury. *Radiology* 252, 816–824. [PubMed: 19567646]
20. Niogi SN, Mukherjee P, 2010. Diffusion tensor imaging of mild traumatic brain injury. *J Head Trauma Rehabil* 25, 241–255. [PubMed: 20611043]
21. Singh M, Jeong J, Hwang D, Sungkarat W, Gruen P, 2010. Novel diffusion tensor imaging methodology to detect and quantify injured regions and affected brain pathways in traumatic brain injury. *Magnetic resonance imaging* 28, 22–40. [PubMed: 19608369]
22. Palacios EM, Yuh EL, Mac Donald CL, Bourla I, Wren-Jarvis J, Sun X, ... & Mukherjee P, 2022. Diffusion Tensor Imaging Reveals Elevated Diffusivity of White Matter Microstructure that is Independently Associated with Long-Term Outcome after Mild Traumatic Brain Injury: A TRACK-TBI Study. *Journal of Neurotrauma* 39, 1–11. [PubMed: 34751584]
23. Schmidt AT, Lindsey HM, Dennis E, Wilde EA, Biekman BD, Chu ZD, Hanten GR, Formon DL, Spruiell MS, Hunter JV, et al. , 2021. Diffusion tensor imaging correlates of resilience following

- adolescent traumatic brain injury. *Cognitive and behavioral neurology* 34, 259–274. [PubMed: 34851864]
24. Galinowski A, Miranda R, Lemaitre H, Martinot MLP, Artiges E, Vulser H, Goodman R, Penttilä J, Struve M, Barbot A, et al. , 2015. Resilience and corpus callosum microstructure in adolescence. *Psychological medicine* 45, 2285–2294. [PubMed: 25817177]
 25. Burt KB, Whelan R, Conrod PJ, Banaschewski T, Barker GJ, Bokde AL, Bromberg U, Büchel C, Fauth-Bühler M, Flor H, et al. , 2016. Structural brain correlates of adolescent resilience. *Journal of Child Psychology and Psychiatry* 57, 1287–1296. [PubMed: 27079174]
 26. Fischer FU, Wolf D, Tüscher O, Fellgiebel A, Initiative ADN, et al. , 2021. Structural network efficiency predicts resilience to cognitive decline in elderly at risk for alzheimer’s disease. *Frontiers in aging neuroscience* 13, 44.
 27. Podwalski P, Szczygiel K, Tyburski E, Sagan L, Misiak B, Samochowiec J, 2021. Magnetic resonance diffusion tensor imaging in psychiatry: A narrative review of its potential role in diagnosis. *Pharmacological Reports* 73, 43–56. [PubMed: 33125677]
 28. Mac Donald CL, Dikranian K, Bayly P, Holtzman D, Brody D, 2007. Diffusion tensor imaging reliably detects experimental traumatic axonal injury and indicates approximate time of injury. *J Neurosci* 27, 11869–11876. [PubMed: 17978027]
 29. Newcombe VF, Correia MM, Ledig C, Abate MG, Outtrim JG, Chatfield D, Geeraerts T, Manktelow AE, Garyfallidis E, Pickard JD and Sahakian BJ, 2016. Dynamic Changes in White Matter Abnormalities Correlate With Late Improvement and Deterioration Following TBI: A Diffusion Tensor Imaging Study. *Neurorehabilitation and neural repair* 30, 49–62. [PubMed: 25921349]
 30. Nelson LD, Temkin NR, Dikmen S, Barber J, Giacino JT, Yuh E, Levin HS, McCrea MA, Stein MB, Mukherjee P, et al. , 2019. Recovery after mild traumatic brain injury in patients presenting to us level I trauma centers: a transforming research and clinical knowledge in traumatic brain injury (track-tbi) study. *JAMA neurology* 76, 1049–1059. [PubMed: 31157856]
 31. Wilson JT, Pettigrew LE, and Teasdale GM, 1998. Structured interviews for the Glasgow Outcome Scale and the extended Glasgow Outcome Scale: guidelines for their use. *J. Neurotrauma* 15, 573–585. [PubMed: 9726257]
 32. Wilson L, Boase K, Nelson LD, Temkin NR, Giacino JT, Markowitz AJ, Maas A, Menon DK, Teasdale G, Manley GT, 2021. A Manual for the Glasgow Outcome Scale-Extended Interview. *J Neurotrauma* 38, 2435–2446. [PubMed: 33740873]
 33. Maas AI, Harrison-Felix CL, Menon D, Adelson PD, Balkin T, Bullock R, Engel DC, Gordon W, Orman JL, Lew HL, et al. , 2010. Common data elements for traumatic brain injury: recommendations from the interagency working group on demographics and clinical assessment. *Archives of physical medicine and rehabilitation* 91, 1641–1649. [PubMed: 21044707]
 34. King NS, Crawford S, Wenden FJ, Moss NE, and Wade DT (1995). The Rivermead Post Concussion Symptoms Questionnaire: a measure of symptoms commonly experienced after head injury and its reliability. *J. Neurol* 242, 587–592. [PubMed: 8551320]
 35. Palacios EM, Martin AJ, Boss MA, Ezekiel F, Chang YS, Yuh EL, Vassar MJ, Schnyer DM, MacDonald CL, Crawford KL, et al. , 2017. Toward precision and reproducibility of diffusion tensor imaging: a multicenter diffusion phantom and traveling volunteer study. *American Journal of Neuroradiology* 38, 537–545. [PubMed: 28007768]
 36. Smith SM, Jenkinson M, Woolrich MW, Beckmann CF, Behrens TE, JohansenBerg H, Bannister PR, De Luca M, Drobnjak I, Flitney DE, et al. , 2004. Advances in functional and structural MR image analysis and implementation as FSL. *NeuroImage* 23, S208–S219. [PubMed: 15501092]
 37. Oishi K, Faria A, Jiang H, Li X, Akhter K, Zhang J, Hsu JT, Miller MI, van Zijl PC, Albert M, et al. , 2009. Atlas-based whole brain white matter analysis using large deformation diffeomorphic metric mapping: application to normal elderly and alzheimer’s disease participants. *Neuroimage* 46, 486–499. [PubMed: 19385016]
 38. Smith SM, & Nichols TE (2009). Threshold-free cluster enhancement: addressing problems of smoothing, threshold dependence and localisation in cluster inference. *Neuroimage*, 44(1), 83–98. [PubMed: 18501637]

39. Benjamini Y, and Hochberg Y 1995. Controlling the false discovery rate: A practical and powerful approach to multiple testing. *J. Royal Stat. Soc* 57:289–300.
40. Nelson LD, Kramer MD, Joyner KJ, Patrick CJ, Stein MB, Temkin N, Levin HS, Whyte J, Markowitz AJ, Giacino J, et al. . 2021. Relationship between transdiagnostic dimensions of psychopathology and traumatic brain injury (tbi): A track-tbi study. *Journal of Abnormal Psychology*.
41. Aldossary NM, Kotb MA, Kamal AM, 2019. Predictive value of early mri findings on neurocognitive and psychiatric outcomes in patients with severe traumatic brain injury. *Journal of affective disorders* 243, 1–7. [PubMed: 30218878]
42. Kurumaji A, Itasaka M, Uezato A, Takiguchi K, Jitoku D, Hobo M, Nishikawa T, 2017. A distinctive abnormality of diffusion tensor imaging parameters in the fornix of patients with bipolar ii disorder. *Psychiatry Research: Neuroimaging* 266, 66–72. [PubMed: 28609689]
43. Zheng KZ, Wang HN, Liu J, Xi YB, Li L, Zhang X, Li JM, Yin H, Tan QR, Lu HB, et al. , 2018. Incapacity to control emotion in major depression may arise from disrupted white matter integrity and ofc-amygdala inhibition. *CNS neuroscience & therapeutics* 24, 1053–1062. [PubMed: 29368421]
44. Jenkins LM, Barba A, Campbell M, Lamar M, Shankman SA, Leow AD, Ajilore O, Langenecker SA, 2016. Shared white matter alterations across emotional disorders: a voxel-based meta-analysis of fractional anisotropy. *NeuroImage: Clinical* 12, 1022–1034. [PubMed: 27995068]
45. Chen G, Guo Y, Zhu H, Kuang W, Bi F, Ai H, Gu Z, Huang X, Lui S, Gong Q, 2017. Intrinsic disruption of white matter microarchitecture in first-episode, drug-naive major depressive disorder: A voxel-based meta-analysis of diffusion tensor imaging. *Progress in Neuro-Psychopharmacology and Biological Psychiatry* 76, 179–187. [PubMed: 28336497]
46. Ghajar J, Ivry R, 2008. The predictive brain state: timing deficiency in traumatic brain injury? *Neurorehabil Neural Repair* 22, 217–27. [PubMed: 18460693]
47. Gatti D, Rinaldi L, Ferreri L, Vecchi T, 2021. The human cerebellum as a hub of the predictive brain. *Brain Sci* 11, 1492. [PubMed: 34827491]
48. Mallott JM, Palacios EM, Maruta J, Ghajar J, Mukherjee P, 2019. Disrupted white matter microstructure of the cerebellar peduncles in scholastic athletes after concussion. *Front Neurol* 10, 518. [PubMed: 31156545]
49. Fields RD, 2015. A new mechanism of nervous system plasticity: activity-dependent myelination. *Nat Rev Neurosci* 16, 756–767. [PubMed: 26585800]
50. Fields RD, Woo DH, Basser PJ, 2015. Glial Regulation of the Neuronal Connectome through Local and Long-Distant Communication. *Neuron* 86, 374–386. [PubMed: 25905811]
51. Sampaio-Baptista C, Johansen-Berg H, 2017. White Matter Plasticity in the Adult Brain. *Neuron* 2017 96, 1239–1251.
52. McCauley SR, Wilde EA, Miller ER, Frisby ML, Garza HM, Varghese R, Levin HS, Robertson CS, McCarthy JJ, 2013. Preinjury resilience and mood as predictors of early outcome following mild traumatic brain injury. *Journal of neurotrauma* 30, 642–652. [PubMed: 23046394]
53. Marwitz JH, Sima AP, Kreutzer JS, Dreer LE, Bergquist TF, Zafonte R, Johnson-Greene D, Felix ER, 2018. Longitudinal examination of resilience after traumatic brain injury: a traumatic brain injury model systems study. *Archives of physical medicine and rehabilitation* 99, 264–271. [PubMed: 28734937]
54. Jorge RE, Robinson RG, Moser D, Tateno A, Crespo-Facorro B, Arndt S, 2004. Major depression following traumatic brain injury. *Archives of general psychiatry* 61, 42–50. [PubMed: 14706943]
55. Nelson LD, Tarima S, LaRoche AA, Hammeke TA, Barr WB, Guskiewicz K, Randolph C, McCrea MA, 2016. Preinjury somatization symptoms contribute to clinical recovery after sport-related concussion. *Neurology* 86, 1856–1863. [PubMed: 27164666]
56. Ahmed S, Venigalla H, Mekala HM, Dar S, Hassan M, Ayub S, 2017. Traumatic brain injury and neuropsychiatric complications. *Indian journal of psychological medicine* 39, 114–121. [PubMed: 28515545]
57. Malaspina D, Goetz RR, Friedman JH, Kaufmann CA, Faraone SV, Tsuang M, Cloninger CR, Nurnberger JI Jr, Blehar MC, 2001. Traumatic brain injury and schizophrenia in members of

- schizophrenia and bipolar disorder pedigrees. *American Journal of Psychiatry* 158, 440–446. [PubMed: 11229986]
58. Hanks RA, Rapport LJ, Waldron Perrine B, Millis SR, 2016. Correlates of resilience in the first 5 years after traumatic brain injury. *Rehabilitation Psychology* 61, 269. [PubMed: 26855130]
 59. Seabury SA, Gaudette É, Goldman DP, Markowitz AJ, Brooks J, McCrea MA, ... & TRACK-TBI Investigators. (2018). Assessment of follow-up care after emergency department presentation for mild traumatic brain injury and concussion: results from the TRACK-TBI study. *JAMA network open*, 1(1), e180210–e180210. [PubMed: 30646055]
 60. Manley GT, Mac Donald CL, Markowitz AJ, Stephenson D, Robbins A, Gardner RC, ... & TED Investigators. (2017). The Traumatic Brain Injury Endpoints Development (TED) initiative: progress on a public-private regulatory collaboration to accelerate diagnosis and treatment of traumatic brain injury. *Journal of neurotrauma*, 34(19), 2721–2730. [PubMed: 28363253]
 61. Bowman K, Matney C, & Berwick DM (2022). Improving traumatic brain injury care and research: a report from the National Academies of Sciences, Engineering, and Medicine. *JAMA*, 327(5), 419–420. [PubMed: 35103760]
 62. Rabinowitz AR, Arnett PA, 2018. Positive psychology perspective on traumatic brain injury recovery and rehabilitation. *Applied Neuropsychology: Adult* 25, 295–303. [PubMed: 29781729]
 63. Howe EI, Langlo KPS, Terjesen HCA, Røe C, Schanke AK, Sjøberg HL, ... & Andelic N (2017). Combined cognitive and vocational interventions after mild to moderate traumatic brain injury: study protocol for a randomized controlled trial. *Trials*, 18(1), 1–11. [PubMed: 28049491]
 64. Maas AI, Menon DK, Adelson PD, Andelic N, Bell MJ, Belli A, ... & Francony G (2017). Traumatic brain injury: integrated approaches to improve prevention, clinical care, and research. *The Lancet Neurology*, 16(12), 987–1048. [PubMed: 29122524]
 65. Savulich G, Menon DK, Stamatakis EA, Pickard JD, & Sahakian BJ (2018). Personalised treatments for traumatic brain injury: cognitive, emotional and motivational targets. *Psychological medicine*, 48(9), 1397–1399. [PubMed: 29636117]
 66. Gaudette E, Seabury SA, Temkin N, Barber J, DiGiorgio AM, Markowitz AJ, Manley GT, and the TRACK-TBI Investigators., in press. Employment and economic outcomes of mild traumatic brain injury patients presenting to US Level 1 trauma centers: A TRACK-TBI Study. *JAMA Netw Open*.
 67. Mikoli A, Polinder S, Helmrich IRR, Haagsma JA, & Cnossen MC (2019). Treatment for posttraumatic stress disorder in patients with a history of traumatic brain injury: a systematic review. *Clinical psychology review*, 73, 101776. [PubMed: 31707182]
 68. Bach M, Laun FB, Leemans A, Tax CM, Biessels GJ, Stieltjes B, & Maier-Hein KH (2014). Methodological considerations on tract-based spatial statistics (TBSS). *Neuroimage*, 100, 358–369. [PubMed: 24945661]

**Figure 1:**

Hypothesized roles of resilience versus DAI on WM microstructural integrity and clinical outcomes after mTBI. Solid boxes represent observed variables; dashed boxes represent unobserved variables. Red arrows and boxes denote negative effects; green arrows/boxes denote positive effects; gold arrows/boxes reflect transitions between observed variables. Larger arrows signify a larger effect. **A.** *What the injury brings to the brain:* The ER and ND patients are assumed to have no difference in preinjury resilience. Differing intensities of DAI are postulated to cause the LPA cluster segregation of the two phenotypes as well as the expected DTI differences (red arrows) that gradually increase between 2 weeks and 6 months postinjury due to group differences in axonal degeneration (red box) that impact clinical outcome. **B.** *What the brain brings to the injury:* The ER and ND patients are assumed to be different in preinjury resilience, but not DAI severity. In this scenario, the initial differences of DTI metrics at 2 weeks are largely due to premorbid differences in resilience and the enlarging differences expected at 6 months are due to adaptive versus maladaptive responses to the mTBI among the ER versus ND patients (green box).

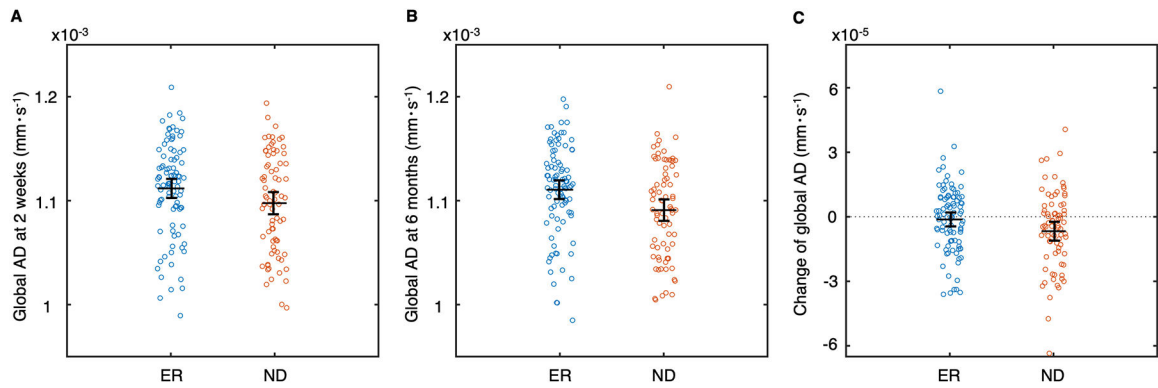


Figure 2:

Global axial diffusivity (AD) comparison between the ER patients (blue dots) and the ND patients (orange dots). The black bars show the mean and its 95% confidence intervals for the group of dots. **A.** ER ($1.112 \pm 0.045 \times 10^{-3} \text{ mm} \cdot \text{s}^{-1}$) had higher AD than ND ($1.098 \pm 0.047 \times 10^{-3} \text{ mm} \cdot \text{s}^{-1}$) at 2 weeks after mTBI. **B.** ER ($1.111 \pm 0.044 \times 10^{-3} \text{ mm} \cdot \text{s}^{-1}$) had higher AD than ND ($1.091 \pm 0.046 \times 10^{-3} \text{ mm} \cdot \text{s}^{-1}$) at 6 months after mTBI. **C.** The longitudinal change of global AD computed as the value at 6 months minus the value at 2 weeks. ND ($-0.671 \pm 1.944 \times 10^{-5} \text{ mm} \cdot \text{s}^{-1}$) showed more negative changes than ER ($-0.124 \pm 1.582 \times 10^{-5} \text{ mm} \cdot \text{s}^{-1}$, not significantly different from zero).

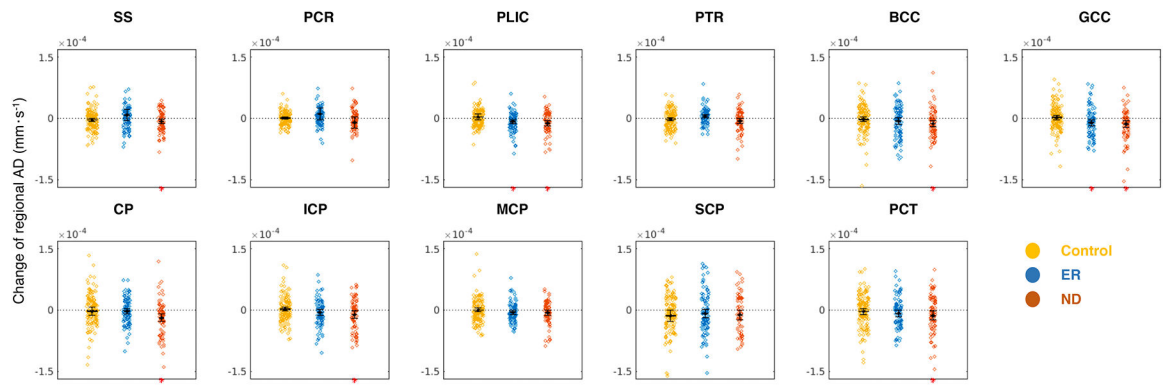


Figure 3:

The longitudinal change of AD computed as the value at the second timepoint minus the value at the first timepoint. A red star on the abscissa denotes a significant longitudinal change after FDR correction. Association tracts: SS - sagittal stratum. Projection tracts: PCR - posterior corona radiata; PLIC - posterior limb internal capsule; PTR - posterior thalamic radiation. Commissural tracts: BCC/GCC - body/genu of corpus callosum. Brainstem and cerebellar tracts: CP - cerebral peduncle; ICP/MCP/SCP -inferior/middle/superior cerebellar peduncle; PCT - pontine crossing tract.

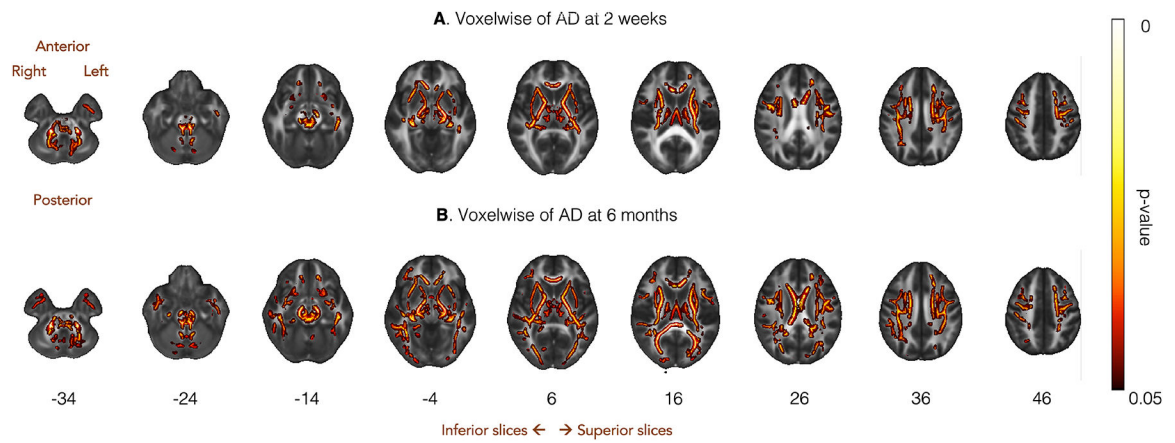


Figure 4:

Voxelwise statistics of AD comparison between ER and ND at 2 weeks (**A** at the top) and 6 months (**B** at the bottom). The colorbar on the right shows the range of p -values from 0.05 to 0 corrected for multiple voxelwise comparisons: red is marginally significant while yellow is highly significant. The statistical significance represents ER patients with higher AD than ND patients in a given WM voxel. In each row, nine slices of the axial view of brain lay out sequentially, with the z -coordinate labeled at the bottom.

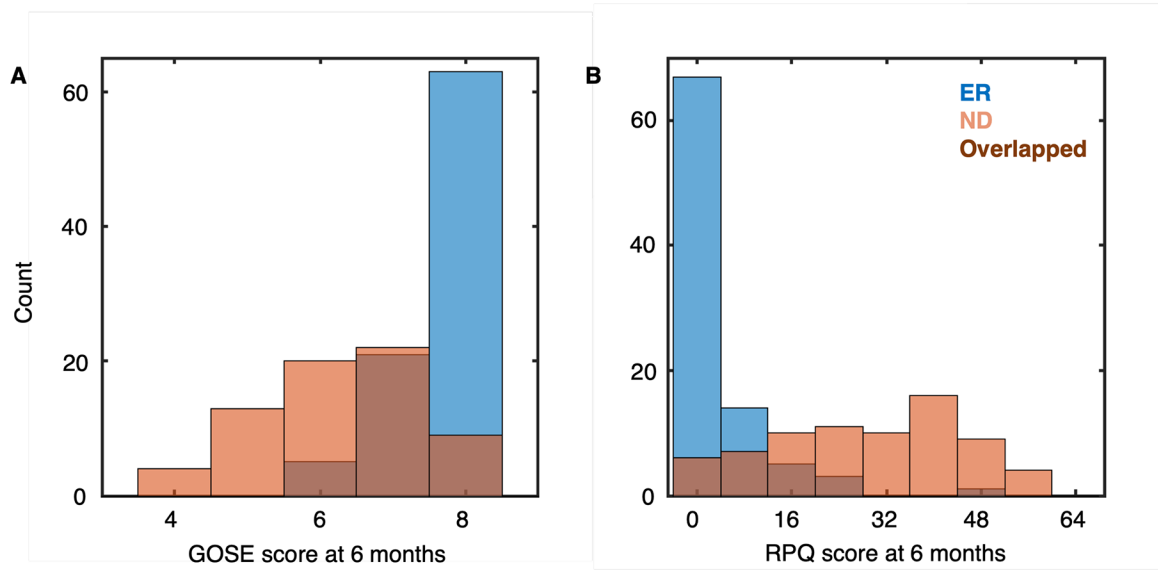


Figure 5: Histograms of outcomes of Glasgow Outcome Scale Extended (GOSE) measure of disability and Rivermead Postconcussion Questionnaire (RPQ) measure of TBI symptoms at six months postinjury, stratified by clinical phenotypes identified at two weeks postinjury. Blue represents the ER cohort and orange the ND cohort.

Table 1:

Differences of DTI regional values at two weeks postinjury between ER and ND patients. For *t*-test, BOLD Cohen's *d* is for $p < 0.05$, a single star is for $p < 0.01$, and a pair of stars is for $p < 0.001$. For the *p*-value, BOLD means the FDR-adjusted *p*-value is also < 0.05 . Association tracts: CGC - cingulum (cingulate gyrus); CGH - cingulum (hippocampus); EC - external capsule; FX and FXST - fornix and stria terminalis; SFO - superior fronto-occipital fasciculus; SLF - superior longitudinal fasciculus; SS - sagittal stratum; UNC - uncinate fasciculus. Projection tracts: ACR/PCR/SCR - anterior/posterior/superior corona radiata; ALIC/PLIC/RLIC - anterior limb/posterior limb/retrolenticular part of internal capsule; CST - corticospinal tract; PTR - posterior thalamic radiation. Commissural tracts: BCC/GCC/SCC - body/genu/splenium of corpus callosum. Brainstem and cerebellar tracts: CP - cerebral peduncle; ICP/MCP/SCP - inferior/middle/superior cerebellar peduncle; ML - medial lemniscus; PCT - pontine crossing tract.

Region	Axial Diffusivity (AD, $\times 10^{-3} \text{ mm}^2 \text{ s}^{-1}$)			Fractional Anisotropy (FA)			Mean Diffusivity (MD, $\times 10^{-3} \text{ mm}^2 \text{ s}^{-1}$)			Radial Diffusivity (RD, $\times 10^{-3} \text{ mm}^2 \text{ s}^{-1}$)					
	$\mu_{ER} \pm \sigma$	$\mu_{ND} \pm \sigma$	<i>p</i>	$\mu_{ER} \pm \sigma$	$\mu_{ND} \pm \sigma$	<i>p</i>	$\mu_{ER} \pm \sigma$	$\mu_{ND} \pm \sigma$	<i>p</i>	$\mu_{ER} \pm \sigma$	$\mu_{ND} \pm \sigma$	<i>p</i>			
CGC	1.19±0.08	1.18±0.08	0.17	0.50±0.04	0.50±0.04	-0.09	0.58	0.73±0.06	0.73±0.05	0.08	0.62	0.51±0.05	0.50±0.05	0.22	0.15
CGH	1.11±0.12	1.10±0.07	0.08	0.44±0.07	0.42±0.07	0.29	0.06	0.73±0.08	0.73±0.07	-0.04	0.77	0.54±0.07	0.56±0.07	-0.22	0.16
EC	1.12±0.06	1.10±0.06	0.34	0.40±0.04	0.39±0.04	0.29	0.06	0.75±0.06	0.75±0.04	0	0.98	0.58±0.04	0.58±0.04	0.07	0.66
FXST	1.71±0.15	1.67±0.14	0.33	0.44±0.05	0.44±0.04	-0.04	0.82	1.13±0.17	1.12±0.15	0.10	0.53	0.85±0.16	0.85±0.16	0.01	0.95
FX	1.24±0.10	1.20±0.07	0.48*	0.51±0.05	0.50±0.05	0.25	0.11	0.77±0.04	0.75±0.05	0.34	0.03	0.53±0.05	0.53±0.05	-0.03	0.86
SFO	1.01±0.09	1.00±0.07	0.15	0.44±0.03	0.44±0.04	0.21	0.18	0.65±0.08	0.64±0.06	0.06	0.72	0.48±0.06	0.47±0.05	0.14	0.36
SLF	1.09±0.05	1.07±0.08	0.33	0.48±0.03	0.48±0.03	0.11	0.46	0.69±0.06	0.69±0.03	-0.02	0.87	0.49±0.05	0.49±0.03	-0.15	0.34
SS	1.25±0.10	1.24±0.06	0.08	0.51±0.04	0.51±0.04	0.14	0.36	0.76±0.06	0.75±0.08	0.13	0.41	0.52±0.04	0.52±0.06	0.10	0.53
UNC	1.20±0.07	1.17±0.08	0.36	0.46±0.06	0.45±0.05	0.22	0.16	0.77±0.04	0.75±0.08	0.26	0.09	0.55±0.07	0.56±0.06	-0.16	0.31
ACR	1.12±0.08	1.12±0.07	0.05	0.46±0.03	0.45±0.05	0.15	0.31	0.72±0.05	0.72±0.04	0.02	0.88	0.52±0.05	0.51±0.05	0.06	0.71
PCR	1.16±0.08	1.15±0.06	0.03	0.47±0.03	0.46±0.04	0.40*	0.009	0.73±0.08	0.74±0.07	-0.09	0.54	0.53±0.04	0.53±0.05	-0.02	0.88
SCR	1.08±0.06	1.06±0.06	0.32	0.48±0.04	0.48±0.04	0.02	0.92	0.66±0.09	0.67±0.04	-0.24	0.12	0.48±0.05	0.47±0.05	0.14	0.36
ALIC	1.20±0.10	1.17±0.08	0.32	0.54±0.04	0.54±0.04	-0.06	0.68	0.69±0.07	0.69±0.06	0.05	0.74	0.45±0.06	0.45±0.04	0	0.98
PLIC	1.29±0.09	1.26±0.07	0.36	0.67±0.04	0.68±0.03	-0.27	0.08	0.67±0.07	0.65±0.04	0.21	0.17	0.37±0.04	0.35±0.04	0.37	0.02
RLIC	1.26±0.09	1.23±0.12	0.28	0.55±0.05	0.55±0.04	0.16	0.29	0.74±0.07	0.73±0.07	0.14	0.36	0.48±0.04	0.48±0.05	0.05	0.73
CST	1.14±0.12	1.13±0.09	0.08	0.58±0.06	0.57±0.06	0.18	0.24	0.66±0.08	0.66±0.07	-0.06	0.72	0.42±0.06	0.43±0.06	-0.10	0.51
PTR	1.30±0.09	1.30±0.06	0.01	0.57±0.04	0.56±0.04	0.19	0.22	0.76±0.04	0.75±0.06	0.06	0.69	0.48±0.05	0.48±0.05	-0.14	0.37
BCC	1.55±0.08	1.53±0.07	0.26	0.64±0.04	0.64±0.04	-0.06	0.69	0.83±0.06	0.82±0.06	0.18	0.25	0.47±0.06	0.46±0.06	0.13	0.40
GCC	1.53±0.09	1.51±0.09	0.26	0.68±0.04	0.67±0.04	0.16	0.31	0.79±0.05	0.78±0.05	0.16	0.30	0.41±0.05	0.42±0.06	-0.06	0.68
SCC	1.52±0.06	1.50±0.08	0.20	0.76±0.03	0.75±0.04	0.25	0.11	0.72±0.04	0.72±0.05	-0.01	0.98	0.31±0.05	0.32±0.05	-0.19	0.22
CP	1.36±0.09	1.34±0.09	0.27	0.65±0.04	0.65±0.04	0.08	0.62	0.72±0.05	0.71±0.05	0.19	0.21	0.40±0.04	0.40±0.06	0.08	0.62

Region	Axial Diffusivity (AD, $\times 10^{-3} \text{ mm}^2 \text{ s}^{-1}$)			Fractional Anisotropy (FA)			Mean Diffusivity (MD, $\times 10^{-3} \text{ mm}^2 \text{ s}^{-1}$)			Radial Diffusivity (RD, $\times 10^{-3} \text{ mm}^2 \text{ s}^{-1}$)						
	$\mu_{\text{ER}} \pm \sigma$	$\mu_{\text{ND}} \pm \sigma$	d	p	$\mu_{\text{ER}} \pm \sigma$	$\mu_{\text{ND}} \pm \sigma$	d	p	$\mu_{\text{ER}} \pm \sigma$	$\mu_{\text{ND}} \pm \sigma$	d	p				
ICP	1.10 \pm 0.05	1.10 \pm 0.05	0.14	0.37	0.51 \pm 0.05	0.50 \pm 0.05	0.26	0.09	0.68 \pm 0.04	0.68 \pm 0.04	-0.03	0.84	0.46 \pm 0.05	0.46 \pm 0.05	0.05	0.75
MCP	1.02 \pm 0.04	1.01 \pm 0.05	0.26	0.09	0.50 \pm 0.03	0.50 \pm 0.03	0.25	0.11	0.63 \pm 0.03	0.63 \pm 0.04	0.15	0.32	0.44 \pm 0.04	0.44 \pm 0.04	-0.07	0.76
SCP	1.42 \pm 0.08	1.38 \pm 0.08	0.50*	0.001	0.59 \pm 0.06	0.58 \pm 0.06	0.17	0.28	0.80 \pm 0.05	0.78 \pm 0.07	0.37	0.02	0.49 \pm 0.07	0.49 \pm 0.06	-0.01	0.94
ML	1.26 \pm 0.06	1.22 \pm 0.13	0.37	0.02	0.60 \pm 0.04	0.59 \pm 0.04	0.26	0.09	0.70 \pm 0.04	0.68 \pm 0.07	0.37	0.02	0.43 \pm 0.04	0.42 \pm 0.05	0.11	0.49
PCT	1.05 \pm 0.08	1.03 \pm 0.07	0.24	0.11	0.49 \pm 0.04	0.47 \pm 0.04	0.34	0.03	0.67 \pm 0.04	0.66 \pm 0.05	0.07	0.66	0.48 \pm 0.05	0.48 \pm 0.05	-0.07	0.64

Table 2:

Differences of DTI regional values at 6 months postinjury between ER and ND patients. For t -test, BOLD Cohen's d is for $p < 0.05$, a single star is for $p < 0.01$, and a pair of stars is for $p < 0.001$. For the p -value, BOLD means the FDR-adjusted p -value is also less than 0.05. WM tract region abbreviations are as in Table 1.

Region	Axial Diffusivity (AD, $\times 10^{-3} \text{ mm}^2 \text{ s}^{-1}$)			Fractional Anisotropy (FA)			Mean Diffusivity (MD, $\times 10^{-3} \text{ mm}^2 \text{ s}^{-1}$)			Radial Diffusivity (RD, $\times 10^{-3} \text{ mm}^2 \text{ s}^{-1}$)						
	$\mu_{ER} \pm \sigma$	$\mu_{ND} \pm \sigma$	d	p	$\mu_{ER} \pm \sigma$	$\mu_{ND} \pm \sigma$	d	p	$\mu_{ER} \pm \sigma$	$\mu_{ND} \pm \sigma$	d	p	$\mu_{ER} \pm \sigma$	$\mu_{ND} \pm \sigma$	d	p
CGC	1.19±0.08	1.18±0.08	0.13	0.40	0.50±0.04	0.50±0.04	0.01	0.93	0.73±0.06	0.73±0.04	0.05	0.75	0.51±0.05	0.50±0.04	0.13	0.40
CGH	1.12±0.12	1.09±0.08	0.31	0.04	0.45±0.04	0.43±0.07	0.27	0.08	0.73±0.07	0.72±0.07	0.16	0.30	0.54±0.07	0.54±0.06	-0.10	0.52
EC	1.12±0.06	1.09±0.06	0.43*	0.005	0.40±0.04	0.39±0.04	0.19	0.22	0.76±0.04	0.75±0.05	0.38	0.01	0.58±0.04	0.58±0.05	0.19	0.21
FXST	1.71±0.17	1.65±0.14	0.36	0.02	0.44±0.04	0.44±0.05	0.08	0.58	1.12±0.18	1.11±0.15	0.08	0.58	0.85±0.16	0.84±0.15	0.09	0.57
FX	1.24±0.09	1.19±0.08	0.62**	<0.001	0.51±0.05	0.50±0.04	0.24	0.12	0.77±0.04	0.75±0.04	0.54**	<0.001	0.53±0.05	0.53±0.04	0.15	0.34
SFO	1.02±0.07	0.98±0.07	0.51*	0.001	0.44±0.04	0.42±0.05	0.29	0.06	0.67±0.05	0.64±0.06	0.46*	0.003	0.48±0.05	0.47±0.07	0.32	0.04
SLF	1.09±0.05	1.07±0.05	0.38	0.01	0.48±0.03	0.47±0.03	0.15	0.34	0.69±0.04	0.68±0.03	0.17	0.26	0.49±0.04	0.49±0.03	0	0.99
SS	1.26±0.07	1.24±0.06	0.36	0.02	0.51±0.04	0.51±0.03	0.20	0.19	0.76±0.08	0.76±0.05	0.02	0.92	0.52±0.06	0.52±0.04	-0.13	0.40
UNC	1.20±0.08	1.17±0.07	0.37	0.02	0.46±0.04	0.44±0.05	0.27	0.08	0.76±0.04	0.76±0.05	0.12	0.44	0.55±0.07	0.56±0.05	-0.20	0.19
ACR	1.12±0.07	1.10±0.10	0.31	0.04	0.45±0.04	0.45±0.05	0.09	0.55	0.72±0.04	0.71±0.05	0.22	0.16	0.52±0.04	0.52±0.04	0.14	0.37
PCR	1.17±0.05	1.14±0.09	0.32	0.04	0.46±0.04	0.46±0.04	0.20	0.19	0.74±0.06	0.74±0.04	-0.05	0.73	0.54±0.06	0.54±0.04	-0.13	0.39
SCR	1.07±0.08	1.06±0.06	0.21	0.17	0.48±0.03	0.48±0.04	0.01	0.94	0.67±0.07	0.69±0.03	-0.03	0.85	0.48±0.05	0.47±0.04	0.09	0.55
ALIC	1.19±0.08	1.16±0.08	0.39	0.01	0.54±0.03	0.54±0.03	0.11	0.48	0.69±0.07	0.69±0.04	-0.01	0.97	0.46±0.05	0.45±0.03	0.08	0.62
PLIC	1.28±0.09	1.25±0.08	0.40	0.01	0.67±0.04	0.67±0.03	-0.07	0.66	0.66±0.07	0.65±0.06	0.25	0.11	0.36±0.05	0.35±0.04	0.24	0.11
RLIC	1.27±0.06	1.23±0.10	0.45*	0.004	0.55±0.03	0.55±0.03	0	0.99	0.75±0.03	0.74±0.04	0.31	0.04	0.49±0.05	0.49±0.04	0	0.99
CST	1.14±0.08	1.12±0.06	0.17	0.28	0.57±0.04	0.58±0.05	-0.11	0.48	0.67±0.05	0.66±0.05	0.26	0.09	0.43±0.06	0.42±0.06	0.08	0.60
PTR	1.31±0.09	1.30±0.06	0.17	0.27	0.57±0.04	0.56±0.04	0.10	0.53	0.76±0.04	0.76±0.04	0.11	0.46	0.48±0.05	0.48±0.05	-0.04	0.81
BCC	1.54±0.08	1.52±0.08	0.35	0.03	0.64±0.04	0.64±0.05	-0.01	0.97	0.83±0.06	0.81±0.06	0.27	0.08	0.47±0.06	0.46±0.06	0.20	0.20
GCC	1.52±0.09	1.50±0.09	0.30	0.05	0.68±0.04	0.67±0.05	0.09	0.55	0.78±0.05	0.77±0.04	0.21	0.18	0.41±0.05	0.41±0.06	-0.01	0.98
SCC	1.52±0.06	1.50±0.07	0.32	0.04	0.75±0.04	0.75±0.03	0.16	0.31	0.72±0.04	0.71±0.05	0.12	0.45	0.32±0.05	0.32±0.05	-0.08	0.62
CP	1.36±0.09	1.32±0.08	0.46*	0.003	0.65±0.04	0.65±0.04	0.04	0.78	0.72±0.05	0.70±0.06	0.41*	0.009	0.40±0.05	0.39±0.05	0.19	0.21
ICP	1.10±0.06	1.09±0.05	0.25	0.11	0.51±0.04	0.50±0.05	0.08	0.59	0.67±0.06	0.67±0.04	-0.05	0.76	0.46±0.06	0.46±0.05	-0.08	0.59
MCP	1.02±0.04	1.00±0.05	0.28	0.07	0.50±0.04	0.50±0.03	0.18	0.25	0.63±0.03	0.62±0.04	0.16	0.31	0.44±0.04	0.44±0.04	0	0.98
SCP	1.41±0.07	1.36±0.12	0.54**	<0.001	0.60±0.05	0.59±0.05	0.09	0.56	0.80±0.06	0.78±0.05	0.31	0.04	0.48±0.08	0.49±0.06	-0.02	0.89
ML	1.25±0.06	1.21±0.13	0.41*	0.009	0.60±0.05	0.59±0.06	0.25	0.11	0.70±0.04	0.78±0.08	0.34	0.03	0.42±0.05	0.42±0.05	0.01	0.93

Region	Axial Diffusivity (AD, $\times 10^{-3}$ mm \cdot s $^{-1}$)		Fractional Anisotropy (FA)		Mean Diffusivity (MD, $\times 10^{-3}$ mm \cdot s $^{-1}$)		Radial Diffusivity (RD, $\times 10^{-3}$ mm \cdot s $^{-1}$)									
	$\mu_{ER} \pm \sigma$	$\mu_{ND} \pm \sigma$	d	p	$\mu_{ER} \pm \sigma$	$\mu_{ND} \pm \sigma$	d	p	$\mu_{ER} \pm \sigma$	$\mu_{ND} \pm \sigma$	d	p				
PCT	1.04 \pm 0.07	1.02 \pm 0.07	0.33	0.03	0.48 \pm 0.03	0.47 \pm 0.04	0.32	0.04	0.67 \pm 0.04	0.66 \pm 0.05	0.08	0.59	0.48 \pm 0.04	0.48 \pm 0.05	-0.08	0.63

Table 3:

Results of repeated measures ANOVA for regions with significant longitudinal changes and/or interactions between phenotype and time. WM tract region abbreviations are as in Table 1.

Region	Factors	Sum. Sq.	D.F.	Mean Sq.	F	p-Value
SS	Time	1.01×10^{-11}	1	1.01×10^{-11}	0.01	0.93
	Phenotype: Time	5.24×10^{-9}	1	5.24×10^{-9}	3.98	0.05
PCR	Time	2.06×10^{-11}	1	2.06×10^{-11}	0.01	0.92
	Phenotype: Time	9.36×10^{-9}	1	9.36×10^{-9}	4.24	0.04
PLIC	Time	8.29×10^{-9}	1	8.29×10^{-9}	28.4	<0.001
	Phenotype: Time	3.55×10^{-10}	1	3.55×10^{-10}	1.22	0.27
PTR	Time	1.13×10^{-11}	1	1.13×10^{-11}	0.04	0.84
	Phenotype: Time	3.12×10^{-9}	1	3.12×10^{-9}	11.5	<0.001
BCC	Time	8.06×10^{-9}	1	8.06×10^{-9}	11.6	<0.001
	Phenotype: Time	8.17×10^{-10}	1	8.17×10^{-10}	1.17	0.28
GCC	Time	1.28×10^{-8}	1	1.28×10^{-8}	19.7	<0.001
	Phenotype: Time	2.02×10^{-10}	1	2.02×10^{-10}	0.31	0.58
CP	Time	1.01×10^{-8}	1	1.01×10^{-8}	14.9	<0.001
	Phenotype: Time	5.52×10^{-9}	1	5.52×10^{-9}	8.12	0.005
ICP	Time	6.07×10^{-9}	1	6.07×10^{-9}	9.92	0.002
	Phenotype: Time	6.86×10^{-10}	1	6.86×10^{-10}	1.12	0.29
MCP	Time	3.00×10^{-9}	1	3.00×10^{-9}	8.83	0.003
	Phenotype: Time	3.36×10^{-11}	1	3.36×10^{-11}	0.10	0.75
SCP	Time	1.66×10^{-8}	1	1.66×10^{-8}	6.81	0.01
	Phenotype: Time	2.44×10^{-9}	1	2.44×10^{-9}	1.00	0.32
PCT	Time	9.97×10^{-9}	1	9.97×10^{-9}	9.99	0.002
	Phenotype: Time	7.32×10^{-10}	1	7.32×10^{-10}	0.73	0.39